INL/CON-24-78635-Revision-0

Fine Temperature Grid Continuous Energy Cross Section Generation for Monte Carlo Analysis of Xe-100 Design

October 2024

Mehmet Turkmen, Paolo Balestra, Matilda Anna Elisabeth Aberg Lindell, Giuseppe Palmiotti, Gokhan Yesilyurt, Nathan George

Changing the World's Energy Future

INL is a U.S. Department of Energy National Laboratory operated by Battelle Energy Alliance, LLC

INL/CON-24-78635-Revision-0

Fine Temperature Grid Continuous Energy Cross Section Generation for Monte Carlo Analysis of Xe-100 Design

Mehmet Turkmen, Paolo Balestra, Matilda Anna Elisabeth Aberg Lindell, Giuseppe Palmiotti, Gokhan Yesilyurt, Nathan George

October 2024

Idaho National Laboratory
Idaho Falls, Idaho 83415

http://www.inl.gov

Prepared for the
U.S. Department of Energy
Under DOE Idaho Operations Office
Contract DE-AC07-05ID14517

Fine Temperature Grid Continuous Energy Cross Section Generation for Monte Carlo Analysis of Xe-100 Design

Mehmet Turkmen[1,*], Matilda A. Aberg Lindell[1], Giuseppe Palmiotti[1], Paolo Balestra[1], Gokhan Yesilyurt[2], Nathan George[2]

[1]Idaho National Laboratory, 1955 N. Fremont Ave. Idaho Falls, ID, 83415, US.
[2]X Energy LLC., 530 Gaither Road, Suite 700 Rockville, MD 20850, US.

ABSTRACT

The standard "A Compact ENDF (ACE)" data libraries used by Monte Carlo based reactor physics codes calculations are provided by Los Alamos National Laboratory (LANL) with a temperature interval mostly of 300 K (e.g. 300 K, 600 K, 900 K) for the cross sections and between 100 K and 200 K for the thermal scattering libraries (TSL). However, some codes such as MCNP lack capability to perform on-the-fly temperature interpolation during simulation both for neutron and TSL cross-sections. To evaluate the impact related to Doppler broadening and spectrum shift associated with TSL changes, this paper explores the potential of adopting a temperature grid finer than the ones contained in the standard data libraries. A 50 K temperature grid was employed to quantify the error in neutronics calculations due to temperature grid resolution. This was achieved by comparing the results of this study (50 K temperature interval) against the results obtained with standard data libraries (>100 K temperature interval). While the adopted grid primarily relies on the ENDF/B-VII.1 library, for neutron cross-sections, it utilizes ENDF/B-VIII.0 library for TSL. The analyses confirmed that the accuracy of neutronics calculations is satisfactory when using a 50 K temperature grid. Notably, adopting a 50 K temperature grid, as opposed to standard libraries or coarser temperature grids, could lead to a difference of no more than a few hundred pcm in δk for both fresh fuel and burnt fuel. The most sensitive reaction type to the temperature grid was as expected identified as the capture cross-section of U-238.

Keywords: Xe-100, Temperature Grid, NQA, Cross section, NJOY

1. INTRODUCTION

Temperature is the main driver on the resonance to lower the peak and broaden the spectral lines at the resonance region, called the Doppler Broadening. This phenomenon is fundamental in understanding the fuel temperature coefficient in thermal reactors and fast reactors. Temperature dependency of neutron cross sections is typically computed using various codes such as ETOE-2 [1], NJOY[2], and PREPRO 2023 [3], which utilize data from ENDF/B version 5 through 7 libraries and is mostly supplied in the tabulated form of continuous or multigroup cross sections, known as the standard ACE data libraries, to Monte Carlo based reactor physics codes such as SERPENT [4], MCNP [5], and MONK [6].

These libraries are the foremost necessity for the reactor physics analyses and are either provided by Los Alamos National Laboratory (LANL) with a temperature interval mostly of 300 K (e.g. 300 K, 600 K, 900 K) for the cross sections and between 100 K and 200 K for the thermal scattering libraries (TSL) such as

* mehmet.turkmen@inl.gov.

the ones coming with the MCNP distribution or provided by different institutes such as Joint Evaluated Fission and Fusion (JEFF) Nuclear Data Library [7] and Japanese Evaluated Nuclear Data Library (JENDL) [8] at certain temperatures. However, the actual temperature within each component (e.g., fuel, clad, gap, coolant) of a reactor varies widely, typically spanning from room temperature at the startup to operating temperature or even to higher temperature in case of an accident. Therefore, the use of standard libraries introduces an indeterminate epistemic uncertainty into modeling and simulation studies originated from the codes such as MCNP, which lack the capability to perform built-in on-the-fly (OTF) temperature interpolation for both neutron and TSL cross-sections. This uncertainty persists even for the codes which have built-in OTF capability due to the complicated fitting techniques employed. Generating such ACE libraries peculiar to each component's temperature would be cumbersome and expensive from the standpoint of computing time, data utilization in simulations, and the number of isotopes to consider in a typical depletion analysis. In this context, this work sought for an applicable fine temperature grid to represent the temperature dependency of cross sections more accurately, which would result in a few pcm difference in δk, to enhance the performance of reactor physics codes.

2. METHODOLOGY

This work, part of the X-energy's Advanced Reactor Demonstration Program (ARDP) project, concentrates on generating cross sections by using the Nuclear Software Quality Assurance-1 (NSQA-1) NJOY, based on a temperature grid finer than the ones contained in the standard libraries released by LANL. The goal of this project is to generate ACE file libraries for use with the Xe-100 MCNP model, by employing a temperature grid finer than the current ones publicly available. The need for this library is related to its use in the Xe-100 reactor design, where a fine temperature distribution is suitable for a very detailed geometrical model that will be used in conjunction with MCNP6. MCNP6 code has no capability to perform on-the-fly temperature interpolation both for cross sections and Thermal Scattering Law (TSL). To evaluate the impact related to Doppler broadening and spectrum shift associated with TSL changes, this paper explores the potential of adopting a temperature grid finer than the ones contained in the standard data libraries. For this, parametric investigations on fresh fuel, burnt fuel and structural materials were performed to determine the grid resolution.

The acceptance criterion for the grid was considered no more than a few hundred pcm in the neutronics model of a unit cell geometry filled with pebbles. In this regard, a temperature grid ranging from 300 to 2000 K space out at intervals of 50 K was employed to quantify the error in neutronics calculations due to temperature grid resolution. The adopted grid primarily relies on the ENDF/B-VII.1 [9] library; however, ENDF/B-VIII.0 [10] is also utilized for isotopes unavailable in ENDF/B-VII.1.

With that in mind, the first step was to assess which isotopes show temperature effects related to resonance Doppler broadening and spectrum shift linked to TSL changes due to temperature variations. The second step was to evaluate the impact of grid temperature in terms of epistemic error introduced by adopting the generated closest temperature ACE file - instead of the publicly available closest temperature ACE file.

This in turn enabled the quantification of possible errors on the neutronic parameters calculated for the neutronic reactor design. The following integral quantities were considered in these investigations: (i) neutron multiplication factor, (ii) spectral indices: $\sigma_f^{U-238}/\sigma_f^{U-235}$, $\sigma_\gamma^{U-238}/\sigma_f^{U-235}$, and $\sigma_{n,\alpha}^{B-10}/\sigma_f^{U-235}$, (iii) kinetic parameters: delayed neutron fraction (β_{eff}) and mean neutron generation time (Λ_{gen}), and (iv) four energy group cross sections with energy limits (in MeV): 1.0e-11, 1.86e-06, 29.0e-06, 0.1, and 19.64.

2.1. Codes Description

NJOY21 v.1.2.3 was used to generate, in ACE format, point-wise nuclear cross sections and related quantities from the evaluated nuclear data in the ENDF format. In this regard, various modules of NJOY code (e.g., MODER, RECONR, BROADR, THERMR, GASPR, UNRESR, HEATR, PURR, LEAPR, and

ACER) were employed, each performing a well-defined processing task. NJOY21 directs the data flow through the other modules. Subsidiary modules for locale, ENDF formats, physics constants, utility routines, and math routines are, for descriptive purposes, grouped within the NJOY21 module. MODER converts ENDF "tapes" back and forth between formatted (i.e., text) and blocked binary modes. RECONR reconstructs point wise (energy-dependent) cross sections from ENDF resonance parameters and interpolation schemes, and effectively decompresses the nuclear data such that other modules may use them. BROADR Doppler-broadens and thins pointwise cross sections to a specified temperature. THERMR produces cross sections and energy-to-energy matrices for free or bound scatterers in the given thermal energy range. GASPR generates gas-production cross sections in the pointwise PENDF format based on basic ENDF cross sections. HEATR generates point-wise heat production cross sections - neutron kinetic energy released in materials (KERMA) factors - and radiation damage production cross sections. PURR is used to prepare unresolved-resonance region probability tables for MCNP. Based on phonon scattering, LEAPR produces thermal scattering data in a format processable via the THERMR module. ACER prepares libraries in ACE format for MCNP. The ACER module is supported by subsidiary modules for the different classes of the ACE format.

Table I gives the input parameters used in each NJOY module. Independent from temperature, these parameters were adapted to cover all the considered isotopes. The LEAPR input parameters were obtained from LEAPR input files provided via the thermal scattering directory found in the ENDF/B-VIII.0 database [11].

Table I. Non-default NJOY input parameters for neutron fast cross-section data.

Module	Input	Value
RECONR	err	0.001
BROADR	errthn	0.001
THERMR	nbin	32
	iin	1
	natom	1
	tol	0.001
	emax	1000.0
HEATR	npk	7
	mtk	302 303 304 402 442 443 444
PURR	nsigz	7
	sigz	1e10 1e5 1e4 1e3 100 10 1
	nladr	32
	nbin	20

The computer code NJOY21 v1.2.3 [2], listed in the INL (Idaho National Laboratory) enterprise architecture (EA) repository, is accepted by INL as qualified scientific and engineering analysis software. As an INL NSQA-1 compliant application, NJOY21 has been verified and validated for use at INL as documented in [12-14]. A benchmark analysis was performed using MCNP 6.2.0 [15] in order to show the disparity/coherency in outputs when comparing the standard libraries that come with each MCNP distribution and the libraries generated by NJOY. In this regard, MCNP6.2, which is listed in the INL EA repository, is also accepted as qualified scientific and engineering analysis software and has been verified and validated for use at INL, as documented in NSQA-1 documentations [16-18]. All the applications are installed and performed on the INL High Performance Computing (HPC) System.

2.2. Test Geometry

For running the calculation, a unit-cell hexagonal close-packed infinite lattice of pebbles, as seen in Figure 1, was used. The material data was obtained from X-energy for the equilibrium core calculations using Very Superior Old Programs (VSOP [19]). The fuel composition was derived by averaging the equilibrium core densities, as obtained via VSOP calculations, over the core volume of the Xe-100 reactor.

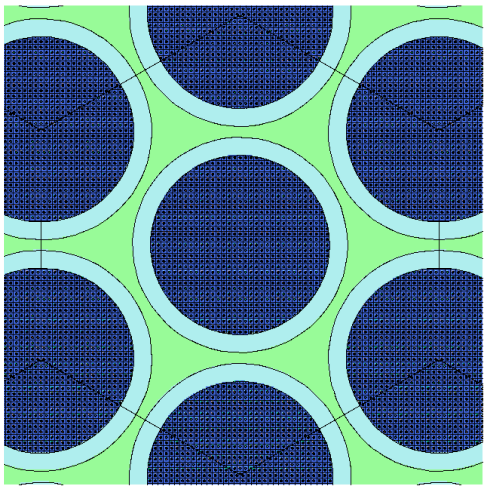

Figure 1. MCNP representation of hexagonal close-packed unit cell with pebbles.

To estimate the point kinetic parameters, KINETICS=YES and PRECURSOR=YES were enabled in the KOPT option. A particular microscopic cross section of an individual isotope - and thus the spectral indices - was calculated using the following equation taken from GDE-594 [20]:

$$\sigma = RR/Flux \tag{1}$$

where *Flux* was obtained using the cell flux card (F4) card, average flux over a cell. *RR* is the reaction rate in the considered cell for the isotope of interest, and was tallied by the F4, along with an appropriate reaction rate tally multiplier card (FM). To obtain energy-dependent flux and reaction rate calculations, an energy (E4) card was appended to both F4 tally cards. $\sigma_{n,\alpha}{}^{B}$ was divided by the abundance of B-10 to obtain $\sigma_{n,\alpha}{}^{B-10}$, due to B-10 being the only contributor to the whole (n,α) reaction up until 10 MeV. The statistical uncertainty in δk calculations is ±3 pcm. δk values are calculated relative to a reference value specifically provided in each table.

2.3. Validation of Generated Cross-Section Libraries

For this investigation, the present study focused on checking the validity of the methodology used in NJOY for generating ACE files for the graphite TSL temperatures that are not provided in the corresponding ENDF/B files. The only TSL investigated was the crystalline graphite TSL in the ENDF/B-VIII.0 library.

Two different scenarios at three different temperatures (600, 900, and 1200 K) were considered when validating the generated cross-section libraries. The investigated cases also aimed to demonstrate the agreement between the standard TSL libraries from LANL ENDF/B-VIII.0 and the generated TSL libraries from LANL ENDF/B-VIII.0. In this respect, the one- and four-group delayed neutron fraction, mean neutron generation time, spectral indices and cross sections for particular U, Pu, and B isotopes were investigated.

3. RESULTS AND DISCUSSION

3.1. Benchmarking Results for Burned Fuel

Based on the test model with burnt fuel, Table II indicates a very small difference between the generated and the standard cross section libraries (XS). Only 2 pcm in δk 1 pcm in δβ, and 1 μs in δΛ was observed at 600 K. Likewise, 5 and 7 pcm in δk were observed at 900 and 1200 K, respectively. The difference appears to slightly increase at elevated temperatures. A comparison of the one- and four-group spectral indices, an example is shown in Table III for 900 K, proved that the generated libraries agree very well with the standard ones. The maximum error was observed to be less than 0.03 % in the fission cross section of U-238.

In the case of TSL comparison, the difference at 600 K showed a TSL effect of about 30 pcm on δk. The difference was seen to increase with increasing temperature (e.g., 50 pcm at 1200 K). The main reason for the greater deviation in TSL compared to XS can be attributed to the recent fixes in LEAPR module of ENDF/B-VIII.0 as indicated in the technical report [21].

Table II. Reactor parameter comparison between the generated and the standard cross-section libraries. Absolute values are provided.

Library	Temp. (K)	δk (pcm)	δβ (pcm)	δΛ (μs)
XS	600	2	1	1
XS	900	5	3	0
XS	1200	7	6	0
TSL	600	30	2	1
TSL	1200	50	12	2

Table III. Percent absolute error (%) in one- and four-energy group spectral indices at 900 K.

Energy Group – Bounds in MeV	$\sigma_f^{U\text{-}238}/\sigma_f^{U\text{-}235}$	$\sigma_\gamma^{U\text{-}238}/\sigma_f^{U\text{-}235}$	$\sigma_{n,\alpha}^{B\text{-}10}/\sigma_f^{U\text{-}235}$
1 of 4: E < 1.0e-11	4.68E-05	1.21E-04	2.74E-04
2 of 4: 1.0e-11 < E < 1.86e-06	1.16E-04	1.13E-06	1.02E-05
3 of 4: 1.86e-06 < E < 29.0e-06	1.83E-02	4.16E-03	6.21E-03
4 of 4: 29.0e-06 < E < 19.64	2.84E-02	1.26E-02	3.37E-03
1 of 4: 0 < E < 19.64	3.08E-03	4.06E-03	2.91E-03

3.2. Temperature Grid Effect on Fresh Fuel

To investigate the temperature grid effect on fresh fuel (C-nat, O-16, U-235, and U-238), we considered four different calculations. The first was at operational temperature of 1050 K, selected as the reference calculation. The second had all isotopes at 900 K, which is the closest matching temperature in the currently available ACE file library. This introduced a temperature error of 150 K. The third one, at 1000 K, corresponds to an adopted temperature grid with 100 K intervals and an associated error of 50 K with respect to the reference temperature. The last one was performed at 1025 K, with an associated error of 25 K and a temperature grid with 50 K intervals. Table IV lists the corresponding results for the kinf calculations. The last column shows the difference in δk with respect to the reference temperature. The 900 K result indicates a significant difference of 1035 pcm, whereas the 1000 K result of 338 pcm is noticeable

but hardly significant. The adopted grid implies an anticipated error of 172 pcm. As expected, the deviation of δk is getting smaller with the use of a finer grid.

For the TSL investigation, only 10 % porosity reactor-grade graphite TSL in the ENDF/B-VIII library was considered. Table V indicates that the temperature grid effect is showing no strong dependency on TSLs, indicating a few pcm in δk at all grids, with statistical uncertainty of ±3 pcm.

Table IV. Temperature grid parametric investigation for the fresh fuel.

Temp. (K)	Grid (K)	Error (K)	δk (pcm)
1050 (ref)	-	-	-
900	300	150	1035
1000	100	50	338
1025	50	25	172

Table V. TSL temperature grid parametric investigation for the fresh fuel.

Temp. (K)	Grid (K)	Error (K)	δk (pcm)
850 (ref)	-	-	-
800	100	50	-1
900	100	50	-1
1000	200	150	-5

3.3. Temperature Grid Effect on Burnt Fuel

To investigate the temperature and temperature grid effects on the burnt fuel, only actinides that were not present in the initial composition (i.e., U-234, U-236, U-237, Np-237, Np-239, Pu-238, Pu-239, Pu-240, Pu-241, Pu-242, Am-241, Am-243, Cm-242, and Cm-244) were added to the fresh fuel composition, with their atomic densities being at the discharge burnup of 164.2 MWd/kg heavy metal for the unit cell model. Actinides with an atomic density of less than 1.0e-6 were not considered in this investigation.

The temperature grid effect was studied via the same approach that was applied to the fresh fuel (i.e., using four different temperature calculations: 900, 1000, 1025, and 1050 K).

Table VI and Table VII illustrate the results obtained for the selected isotopes. For the 50 K grid, only U-238 had a noticeable level of error (116 pcm). Although Pu-240 had some visible errors for the 300 and 100 K grids, it was within statistical uncertainty for the 50 K one. Other isotopes were all within statistical uncertainty for each of the different temperature grids.

Table VI. Temperature grid parametric investigation for some selected actinides in the burnt fuel.

Temp. (K)	Grid (K)	Error (K)	δk (U-235)	δk (U-236)	δk (U-238)
1050	-	-	-	-	-
900	300	150	-	11	1038
1000	100	50	0	6	291
1025	50	25	3	4	116

Table VII. Temperature grid parametric investigation for some selected actinides in the burnt fuel (Cont'd).

Temp. (K)	Grid (K)	Error (K)	δk (Pu-239)	δk (Pu-240)	δk (Pu-242)	δk (Cm-244)
1050	-	-	-	-	-	-
900	300	150	4	81	4	-3
1000	100	50	4	23	-1	-3
1025	50	25	1	10	1	0

3.4. Temperature Grid Effect on Structural Materials

A specific composition was created to investigate the temperature and temperature grid effects on isotopes consisting of structural materials based on their spectrum-dependent absorption cross sections. The composition was added into the fuel composition. No light isotopes or impurities were considered for the work. The temperature effect was studied for elements with an atomic density of 1.0e-02, including Al (Al-27), Cr (Cr-52), Cu (Cu-63 and Cu-65), Fe (Fe-56 and Fe-58), Mn (Mn-55), Mo (Mo-92, Mo-94, Mo-95, Mo-97, Mo-98, and Mo-100), Ni (Ni-58), Nb (Nb-93), Ti (Ti-48), and V (V-51).

Table VIII and Table IX show the results of the temperature investigation. Apparently, of the isotopes, only three are impacted by temperature: Ni-58, Mo-95, and Mo-100. For the 50 K temperature grid, only Mo-95 had some noticeable error (27 pcm). The other isotopes were all within statistical uncertainty for each of the different temperature grids, apart from Mo-100, which had a mere 9 pcm error for the 300 K degrees grid.

Table VIII. Temperature grid parametric investigation for some selected actinides in the burnt fuel.

Temp. (K)	Grid (K)	Error (K)	δk (Cu-63)	δk (Fe-58)	δk (Ni-58)	δk (Nb-93)
1050	-	-	-	-	-	-
900	300	150	-1	1	-6	7
1000	100	50	-2	1	-5	1
1025	50	25	0	-4	-7	-1

Table IX. Temperature grid parametric investigation for some selected actinides in the burnt fuel (Cont'd).

Temp. (K)	Grid (K)	Error (K)	δk (Mo-95)	δk (Mo-97)	δk (Mo-98)	δk (Mo-100)
1050	-	-	-	-		-
900	300	150	119	5	-2	20
1000	100	50	46	-2	-4	10
1025	50	25	27	1	-1	9

4. CONCLUSIONS

The analyses confirmed that the accuracy of neutronics calculations is satisfactory when using a 50 K temperature grid. It was noted that adopting a 50 K temperature grid instead of coarser temperature grids or the standard libraries could lead to a difference of no more than a few hundred pcm in δk regarding fresh

fuel. The reaction type that was most sensitive to the temperature grid was as expected the capture cross section of U-238. Meanwhile, the TSL libraries yielded a difference of around a few pcm in δk.

In the case of burnt fuel with actinides included, the outcomes were similar to those for fresh fuel. Of the various structural isotopes, Mo-95 was identified as being the most sensitive to the temperature grid - a difference of about 30 pcm in δk - while the rest remained within the three-sigma statistical error. Thus, the proposed temperature grid was considered sufficient for use in neutronics calculations.

Finally, using the NJOY parameters specified in Section II.A, the benchmark outcomes indicated that accurately generated cross sections and TSL libraries aligned well with the standard LANL libraries, yielding a relative error of less than 0.04 %. To further minimize this error, one can utilize finer input parameters such as an increased number of resonance ladders and sigma zeros, at the expense of a substantial increase in the computational cost of generating cross-section libraries for individual isotopes.

All in all, even though adopting an even finer temperature grid (e.g., a 25 K temperature grid) would further enhance the accuracy of neutronics calculations, it would also substantially increase the database size, thereby posing challenges in terms of handling the data and generating the cross-section libraries.

ACKNOWLEDGMENTS

This manuscript was authored by Battelle Energy Alliance, LLC under Contract No. DE-AC07-05ID14517 with the U.S. Department of Energy. The U.S. Government retains and the publisher, by accepting the article for publication, acknowledges that the U.S. Government retains a nonexclusive, paid-up, irrevocable, worldwide license to publish or reproduce the published form of this manuscript, or allow others to do so, for U.S. Government purposes. This research used resources of the Idaho National Laboratory High Performance Computing (INL HPC) system, which is supported by the Office of Science of the U.S. Department of Energy under Contract No. DE-AC07-05ID14517. This research was funded by the U.S. Department of Energy Office of Clean Energy Demonstration (OCED) and managed by the National Reactor Innovation Center (NRIC).

REFERENCES

[1] C. Lee, H. Park, and Z. Zhong, "Recent Updates in ETOE-2 and MC²-3," United States, 2021. [Online]. Available: https://www.osti.gov/biblio/1830755

[2] A. C. Kahler, D. W. Muir, R. M. Boicourt, J. L. Conlin, and W. Haeck, "The NJOY Nuclear Data Processing System, Version 2016," Los Alamos National Laboratory, LA-UR-17-20093, 2019. [Online]. Available: https://github.com/njoy/NJOY2016-manual/raw/master/njoy16.pdf

[3] D. E. Cullen, "PREPRO 2023: ENDF/B Pre-processing Codes," International Atomic Energy Agency, IAEA-NDS-0241, June 2023. [Online]. Available: https://www-nds.iaea.org/public/endf/prepro/

[4] J. Leppänen, M. Pusa, T. Viitanen, V. Valtavirta, and Toni Kaltiaisenaho, "The Serpent Monte Carlo code: Status, development and applications in 2013," *Annals of Nuclear Energy,* vol. 82, pp. 142-150, 2015, doi: https://doi.org/10.1016/j.anucene.2014.08.024.

[5] J. A. Kulesza *et al.*, "MCNP Code Version 6.3.0 Theory & User Manual," Los Alamos National Laboratory, LA-UR-22-30006, Rev.1, 2022. [Online]. Available: https://www.osti.gov/servlets/purl/1889957

[6] S. D. Richards *et al.*, "MONK and MCBEND: Current status and recent developments," *Annals of Nuclear Energy,* vol. 82, pp. 63-73, 2015, doi: https://doi.org/10.1016/j.anucene.2014.07.054.

[7] A. Santamarina *et al.*, "The JEFF-3.1.1 Nuclear Data Library," Nuclear Energy Agency, ISBN 978-92-64-99074-6, 2009. [Online]. Available: https://www.oecd-nea.org/jcms/pl_14470/the-jeff-3-1-1-nuclear-data-library?details=true

[8] O. Iwamoto *et al.*, "Japanese evaluated nuclear data library version 5: JENDL-5," *Journal of Nuclear Science and Technology,* vol. 60, no. 1, pp. 1-60, 2023/01/02 2023, doi: 10.1080/00223131.2022.2141903.

[9] M. B. Chadwick *et al.*, "ENDF/B-VII.1 nuclear data for science and technology: Cross sections, covariances, fission product yields and decay data," *Nuclear Data Sheets,* vol. 112, no. 12, pp. 2887-2996, 2011, doi: 10.1016/j.nds.2011.11.002.

[10] D. A. Brown *et al.*, "ENDF/B-VIII.0: The 8th Major Release of the Nuclear Reaction Data Library with CIELO-project Cross Sections, New Standards and Thermal Scattering Data," *Nuclear Data Sheets,* vol. 148, pp. 1-142, 2018, doi: https://doi.org/10.1016/j.nds.2018.02.001.

[11] ENDF/B-VIII.0 Database. https://www.nndc.bnl.gov/endf-b8.0/zips/ENDF-B-VIII.0_thermal_scatt.zip (accessed.

[12] INL, "Software Test Plan for NJOY21 Application," Idaho National Laboratory, PLN-6896 Rev. 0, 2023.

[13] INL, "System Requirements and Traceability Matrix for NJOY21 Application," Idaho National Laboratory, SPC-70751 Rev. 0, 2023.

[14] INL, "System Requirements Specification for NJOY21 Application," Idaho National Laboratory, SPC-70750 Rev. 0, 2023.

[15] C. J. Werner *et al.*, "MCNP User's Manual Code Version 6.2," Los Alamos National Laboratory, LA-UR-17-29981, 2017. [Online]. Available: http://permalink.lanl.gov/object/tr?what=info:lanl-repo/lareport/LA-UR-17-29981

[16] INL, "Software Test Plan for MCNP," Idaho National Laboratory, PLN-6902, Rev. 0, 2023.

[17] INL, "Verification and Validation of MCNP for C730," Idaho National Laboratory, ECAR-8068, Rev. 0, 2024.

[18] INL, "System Requirements Specification for MCNP," Idaho National Laboratory, SPC-70757, Rev. 0, 2023.

[19] E. Teuchert, U. Hansen, and K. A. Haas, "VSOP-computer code system for reactor physics and fuel cycle simulation," Kernforschungsanlage Juelich G.m.b.H. (Germany, F.R.). Inst. fuer Reaktorentwicklung, Germany, Juel--1649, 1980. [Online]. Available: http://inis.iaea.org/search/search.aspx?orig_q=RN:11562514

[20] GDE-594, "Experiment Design and Analysis Guide - Neutronics & Physics " Idaho National Laboratory, 2017.

[21] D. K. Parsons and C. A. Toccoli, "Re-Release of the ENDF/B VIII.0 S(α,β) Data Processed by NJOY2016," Los Alamos National Laboratory, LA-UR-20-24456, June 22 2020.